SCIENTIFIC REPORTS

OPEN

Acoustic-like dynamics of amorphous drugs in the THz regime

E. A. A. Pogna[1], C. Rodríguez-Tinoco[2], M. Krisch[3], J. Rodríguez-Viejo[2,4] & T. Scopigno[1]

[1]Dipartimento di Fisica, Universitá di Roma ''La Sapienza'', I-00185, Roma, Italy, [2]Nanomaterials and Microsystems Group, Physics Department, Universitat Autònoma de Barcelona, ES 08193, Bellaterra, Spain, [3]European Synchrotron Radiation Facility, Bote Postal 220, F-38043 Grenoble, France and, [4]MATGAS 2000 AIE, Campus UAB, 08193 Bellaterra, Spain.

The high frequency dynamics of Indomethacin and Celecoxib glasses has been investigated by inelastic x-ray scattering, accessing a momentum-energy region still unexplored in amorphous pharmaceuticals. We find evidence of phonon-like acoustic dynamics, and determine the THz behavior of sound velocity and acoustic attenuation. Connections with ordinary sound propagation are discussed, along with the relation between fast and slow degrees of freedom as represented by non-ergodicity factor and kinetic fragility, respectively.
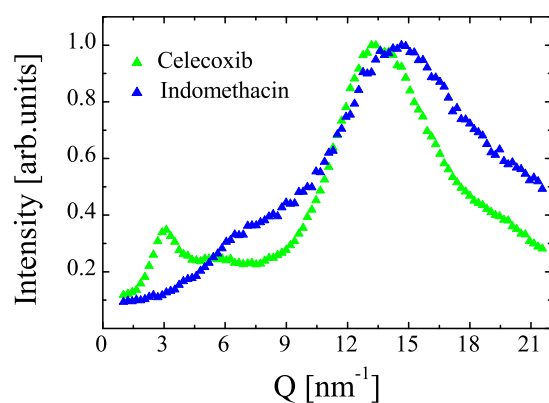
Recently, the preparation of pharmaceutical substances in glassy state has been proven successful in improving their therapeutic performances[1,2]. The glassy state offers advantages such as higher solubility, dissolution rate, and sometimes better compression properties as compared to the crystalline form. As models of amorphous drugs, Indomethacin and Celecoxib are of particular interest because in their crystalline form they are both limited by poor water-solubility[3–7]. At the microscopic scale, the glassy state is characterized by the lack of long range structural order and it exhibits thermodynamical and transport properties consistently different from those of the crystalline phase. Extensive research in the past decades has demonstrated that all glasses, without sensitivity to their composition, exhibit identical thermodynamic anomalies, the most notorious being the thermal conductivity plateau and specific heat C(T) excess over the Debye expectation in the low-temperature regime, near 10 K[8]. These universal features are generally ascribed to an excess in the density of vibrational states over the trend $\propto \omega^2$ predicted by the Debye model for crystalline solids[9], conventionally called Boson peak (BP). The Boson peak is experimentally observed in all glasses by Raman[10,11] and inelastic neutron scattering[12], and numerically reported by molecular dynamics simulations and in focus of several theoretical efforts[13–17]. The anomalies of the density of state can be, in turn, inferred from the peculiarities of the frequency spectra of atomic vibrations. While the vibrational properties of the crystalline state are well rationalized in terms of phonon modes, those of the glassy state are still a matter of intense debate. Due to the lack of translational invariance, even in ''harmonic'' glasses, the vibrational eigenstates are distinctly different from ideal plane waves. Nevertheless, since they exhibit propagating behavior in the long wavelength limit, they are conventionally described by the phonon-like formalism inherited from crystals. The development of high resolution (meV) inelastic x-ray scattering (IXS)[18] has opened the possibility of investigating acoustic dynamics of glasses in the BP region. A sizable library of IXS observations indicates the existence of vibrational excitations characterized by well defined dispersion curves resembling those of the crystalline counterparts, though with distinctive properties influenced by disorder, such as the complex sound attenuation dependencies on temperature and frequency. Acoustic attenuation in glasses is indeed determined by the interplay of different mechanisms[19–21]. In the high (THz) frequency regime, i.e. at acoustic wavelengths comparable to the mean interparticle distances, the temperature independent effect of structural disorder dominates and it is responsible for a progressive localization of acoustic modes occurring as consequence of scattering. One criterion to determine the localization threshold is the Ioffe-Regel criterion, i.e. the equivalence between the excitation mean free path and the dominant excitation wavelength. It has been proposed that the Ioffe-Regel condition on longitudinal vibrational modes coincides with the BP position[22], although this is not generally accepted[23] and it has been pointed out that the criterion should be rather applied to the transverse acoustic branch[16,24–26]. In recent years, the idea that vibrational properties of glasses may be related to the liquid side of the glass formation process has gradually emerged. Specifically, a strong correlation between the temperature dependence of the non-ergodicity factor, and the kinetic fragility m of the corresponding liquids has been proposed as universal feature of glass formation[27–29]. The former represents the long time limit of the normalized density-density correlation function *in the glass*, it is therefore a measure of the decorrelation introduced by the fast vibrational dynamics or, equivalently, of the residual correlation over the ergodicity of
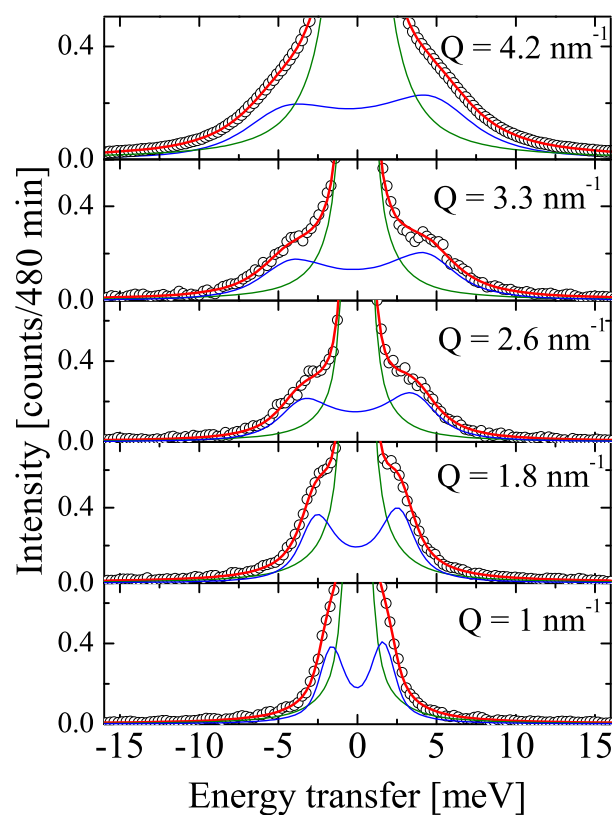
the underlying liquid phase. The latter is the steepness of the (super-cooled) liquid viscosity measured at the glass transition, i.e. as the diffusive motion of the liquid state slows down[30,31]. Liquids whose fragility m ranges from 17 to 30 are classified as strong liquid (Arrhenius-like behavior of viscosity), such as silica, whereas fragility values from 100 to 150 correspond to so-called fragile systems (T-dependent and non-Arrhenius like behavior of viscosity), such as o-terphenyl. Remarkably, the proposed correlation of kinetic fragility to the non-ergodicity factor in the low temperature T = 0 limit can be used to introduce a definition of fragility uniquely from glass properties away from T_g. Fragility correlates, in turn, to several other essential properties in the glass, such as molecular mobility below T_g that is believed to be an important parameter to explain the physical stability of some amorphous compounds towards crystallization[32,33]. In fragile liquids the molecular mobility changes rapidly approaching T_g and this is why strong glass-formers are considered to be more stable than fragile ones[31], a property well known to glass blowers since a long time. Understanding the critical factors governing the crystallization tendency of organic compounds is of fundamental interest when assessing the feasibility of an amorphous formulation for pharmaceuticals. The dependence on the method of preparation has been consistently explored, for example, determining the crucial role played by the cooling rate in glasses synthesized by quench cooling of the liquid[34]. Many amorphous drugs, IMC and CXB included, are characterized by large values of kinetic fragility that classify them as fragile materials and they show a large tendency towards crystallization that prevents their continuous utilization in the amorphous form[35,36]. High frequency vibrational properties of amorphous drugs are still unexplored. We report here IXS measurements on two pharmaceutical glasses with different kinetic fragility, Indomethacin and Celecoxib. Specifically, we determine the longitudinal sound dispersion, the high frequency acoustic attenuation and the non-ergodicity factor, discussing the eigenmodes localization and their connection with mass diffusivity.

Results

The x-ray diffraction measurements on Indomethacin (IMC) and Celecoxib (CXB), detected with a photodiode embedded in the inelastic analyzers bench, show a broad main peak centered at $Q_p^{CXB} = 13.2 \, nm^{-1}$ and $Q_p^{IMC} = 14.7 \, nm^{-1}$, confirming the amorphous nature of the samples (see Fig. 1). A selection of inelastic x-ray scattering spectra of IMC in the glassy state are shown in Fig. 2 at five fixed values of exchanged momentum Q. They are dominated by an intense elastic feature due to the non-ergodicity of the glass, i.e. to density fluctuations frozen by the structural arrest. At both sides of the elastic component, well defined inelastic peaks are observed at


Figure 2 | Selection of room temperature inelastic x-ray scattering spectra of glassy Indomethacin at fixed exchanged momentum Q along with the best fits (red line) described in section Methods. The energy resolution (green line) normalized to the elastic peak (elastic component) is also reported, while the blue line corresponds to the inelastic, damped harmonic oscillator contribution. The experimental error is within the symbol.

Figure 1 | X-ray diffraction patterns of Indomethacin (blue triangles) and Celecoxib glasses (green triangles) as function of the exchanged wave vector Q, normalized to the intensity of the main peak, measured at room temperature 300 K using an incident energy E = 23.725 KeV.

finite energy transfer. The energy position $\hbar\Omega$ of the inelastic peaks corresponds to the energy of the acoustic modes of momentum Q, while the peak width gives access to the life time of density fluctuations , i.e. to the sound attenuation $\Gamma(Q)$. The IXS spectrum can be modeled by a delta function, describing the elastic component, combined with the power spectrum of a damped harmonic oscillator (DHO, corrected to account for the detailed balance condition) representing the inelastic scattering. Both contributions have been convoluted with the instrument response function (green line in Fig. 2, for further details see the Methods section) to correctly reproduce the experimental data. We note that the inelastic contributions to the total scattered intensity due to the Brillouin inelastic scattering from vibrational density fluctuations are well reproduced (blue line in Fig. 2). The energy position of the Brillouin component increases with exchanged momentum Q, testifying the propagating nature of the probed excitations. This general finding proves the existence of THz hypersonic waves in amorphous IMC and CXB. Since only one inelastic contribution is resolved at each Q value, the vibrational excitations can unambiguously be ascribed to a single longitudinal acoustic phonon branch. The inelastic component becomes less and less visible as the exchanged momentum increases, due to an increase of the acoustic attenuation (broadening of the inelastic features) and to the increase of the elastic component which follows the static structure factor S(Q) (see Fig. 1). The energy dispersion curves, $\hbar\Omega(Q)$, of the longitudinal acoustic phonon are linear in the long wavelength-limit Q $\leq$ 3 nm^{-1}; they then bend down reaching a maximum at Q around half of Q_p, highly suggestive of the existence of a pseudo-Brillouin zone (see Fig. 3). The plateau in the phonon dispersion of Indomethacin indicates the end of the propagating behavior while in the Celecoxib the group velocity remains finite
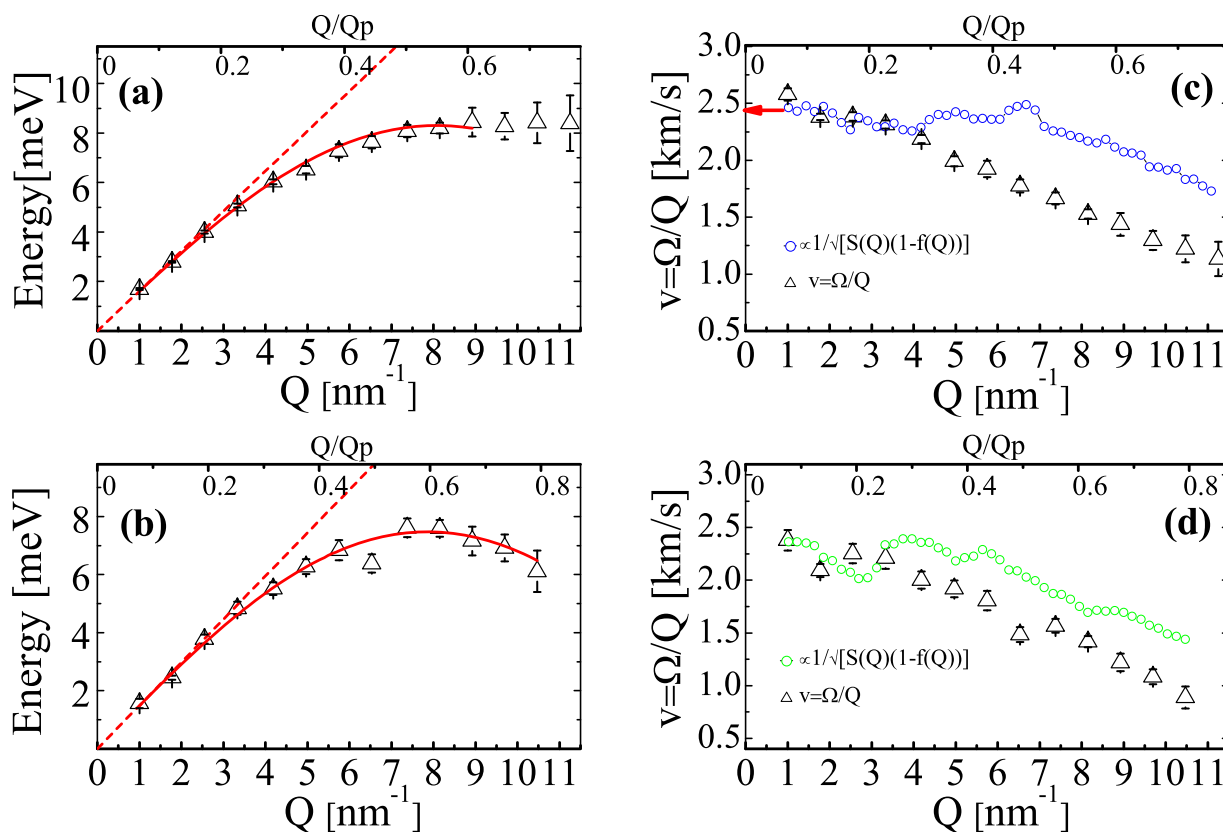
Figure 3 | Energy peak position $\hbar\Omega(Q)$, as obtained from the fit of the data to eq.6, for (a) Indomethacin (b) Celecoxib measured as function of exchanged momentum Q. The parameter $\Omega(Q)$ corresponds to the maximum of the longitudinal current that is $\omega^2/Q^2 S(Q,\omega)$. The bottom axes represent the exchanged momentum Q; the top axes show Q/Q_p where Q_p is the maximum of the XRD patterns. Apparent sound velocity $v = \Omega/Q$ along with its expected hydrodynamic Q-dependency (see Eq.1) (c) Indomethacin (d) Celecoxib.

up to 0.8 Q_p. The acoustic attenuation Γ shows for both samples a power law dependence on the acoustic frequency $\Omega(Q)$ compatible with the quadratic law found in different classes of glassy systems in a similar frequency regime (see Fig. 4).

Discussion

The interest in amorphous form of Indomethacin and Celecoxib is relatively recent and there is no report of previous characterization of the hypersonic sound propagation. In order to investigate the sound velocity, the energy dispersion curves reported here have been analyzed with a sinusoidal fitting function (solid red line in Fig. 3). In the case of Indomethacin we used Q values up to $Q/Q_p = 0.6$ because for higher exchanged momentum there is no longer any significant dispersion. From the linear fit of the dispersion curves in the limit $Q\to 0$ (dashed red line in Fig. 3) the longitudinal sound velocity in Indomethacin and Celecoxib has been estimated to be equal to 2460 m/s and 2214 m/s, respectively. In the case of IMC glass, the extrapolated value agrees very well with previous Brillouin Light Scattering measurement at few GHz[37] (red arrow in panel c of Fig. 3), while, unfortunately, a similar comparison for CXB is not possible due to the lack of any sound velocity data. The sound velocity dispersion $v_a(Q) = \frac{\Omega(Q)}{Q}$ is reported in Fig. 3 and compared to the long wavelength, hydrodynamic limit, derived according to the generalized Langevin equation adapted to the glassy state, i.e. taking into account the non-ergodicity factor f(Q) (estimated via Eq.3)[38-40]. Accordingly, for an harmonic glassy system, the Q-dependency of $v_a(Q)$ reads:

$$v_a \propto \sqrt{\frac{1}{S(Q)(1-f(Q))}} \qquad (1)$$

normalised in Fig. 3 to the $Q \to 0$ limit. The model describes the experimental decreasing trend upon approaching the pseudo Brillouin zone; both systems verify quite well the prediction till $0.2Q_p$, indicating that, within our experimental accuracy, we do not detect anomalous (positive or negative) dispersion effects else reported in different glasses[26,41-43,45]. The discrepancy with Eq.1, observed for further momentum increase, is most likely due to the Q-dependency of the (unknown) form factor, leading to the underestimation of S(Q).

As we pointed out, the microscopic disorder induces the localization of vibrational excitations signaled by the Ioffe-Regel crossover. The onset frequency Ω_{IR} is defined as the inverse of the decay time of the plane wave $\tau = \frac{1}{\pi \Gamma}$ such that:

$$\Gamma_{IR} = \frac{\Omega_{IR}}{\pi} \qquad (2)$$

The Ioffe-Regel crossover frequencies determined by longitudinal vibrational excitations in IMC and CXB are found at $\Omega_{IR}^{IMC} = 2.3$ meV and $\Omega_{IR}^{CXB} = 1.4$ meV, respectively (see Fig. 4). These values are compatible with that of other molecular glasses[22]. Remarkably, in the case of IMC and CXB the Ioffe-Regel crossover determined for longitudinal waves does not correspond to spatial localization of vibrational excitations since we observe the existence of low energy dispersive excitations up to almost $\hbar\omega = 8$ meV ($Q = 7$ nm^{-1}). According to simulations on vitreous silica[44], the Ioffe-Regel crossover frequency for vibrational excitations may not correspond to mode localization but rather to the change into diffusive, spatially extended states, resulting from the mixing of propagating phonons with localized vibrational modes. As discussed in the introduction,
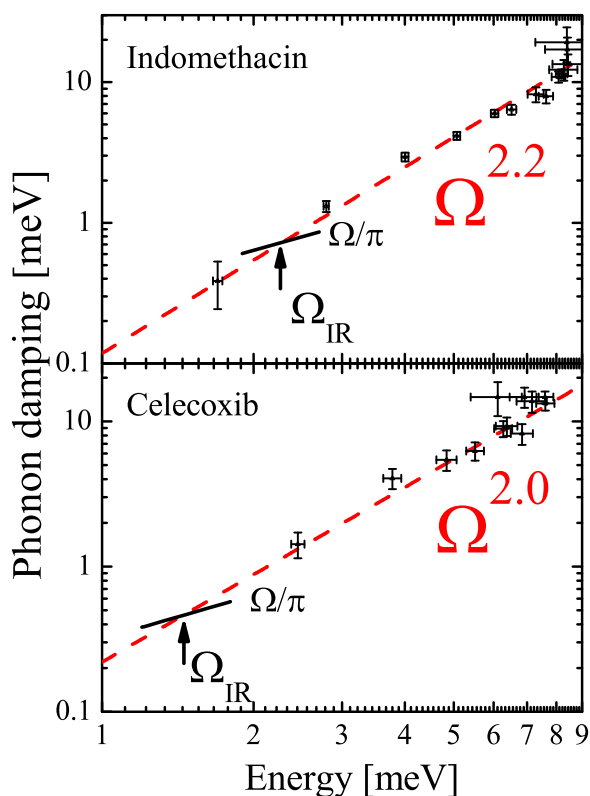
Figure 4 | Acoustic attenuation Γ of Indomethacin (upper panel) and Celecoxib (lower panel) as function of energy of the acoustic mode $\hbar\Omega$ on a log log scale, along with the best fit result utilizing a power law of exponent 2.2 for IMC and 2.0 for CXB. The Ioffe-Regel condition Ω_{IR} is determined from the crossing frequency of the attenuation curves with the function Ω/π.

the sound attenuation in glasses displays a complex behavior when studied over an extended wavelength range. In this study, a nearly quadratic dependence $\Gamma = a\, v^{2.2}$ in the THz domain is reported for IMC with a coefficient $a = 0.7\ THz^{-1}$. Quadratic dependencies with different coefficients for the low frequency, anharmonic, behavior and the high frequency, disorder dominated, regime have already been reported in literature in strong glass-formers[21,46], with an higher coefficient for the latter. Interestingly, from a previous Brillouin scattering study in IMC in the GHz range at 325 K one would get a coefficient 13.5 THz^{-1} [37], i.e. the opposite trend is observed, suggesting a larger contribution from the anharmonicity. In order to pursue the correlation between mechanical properties and thermodynamical features of the two investigated drugs, the non-ergodicity factor $f(Q, T)$ is estimated, according to eq.3, as the ratio between the elastic and total intensity of IXS spectra:

$$f(Q, T) = \frac{I_{el}}{I_{el} + I_{inel}} \qquad (3)$$

Invoking the harmonic approximation for the vibrational dynamics, the temperature dependence of the non-ergodicity factor in the low Q region can be described[27] as:

$$f(Q \to 0, T) = \frac{1}{1 + \alpha \frac{T}{T_g}} \qquad (4)$$

where the coefficient α contains all the microscopic details of the system. From equations 3 and 4 the coefficient α can be written as:

$$\alpha = \frac{I_{inel}}{I_{el}} \frac{T_g}{T} \qquad (5)$$

The estimated parameter α of IMC was compared to that of several glassy systems and the proposed correlation with kinetic fragility was verified (see Fig. 5). IMC is usually classified as fragile material, though determination of m by different methods (dielectric spectroscopy, calorimetry and diffusivity) are scattered in the range $60 < m < 79$[3,47,48]. Based on the correlation with the non-ergodicity factor the extrapolated fragility of IMC is $m_\alpha = 73$, a value that falls within the range of previous estimations, very close to the calorimetry measurement. A reliable estimate of the non-ergodicity factor in Celecoxib could not be obtained due to the pre-peak in the static form factor (see Fig. 1). The latter is responsible for an additional contribution to the quasi elastic scattering preventing the determination of the non-ergodicity factor with the aforementioned method. Summing up, this study provides a complete characterization of the THz dynamics of two prototypical pharmaceuticals prepared in the glassy state. Our results demonstrate the existence of acoustic-like, hypersonic vibrational excitations with a well defined dispersion relation and disorder dominated damping. The measure of the non-ergodicity factor, as determined by IXS spectra, is utilized for assessing the fragility of the glass phase. On the basis of Ref. 32, we anticipate that the latter, in turn, may influence the molecular mobility of the supercooled phase, a parameter that has been proposed to rule the glass-forming ability of a given compound, and thus that has fundamental importance for amorphous pharmaceuticals.

Methods

Indomethacin (99% purity, T_g = 315 K and T_m (γ form) = 428 K) and Celecoxib (98% purity with T_g = 326 and T_m = 435 K) crystalline powders were purchased from Sigma-Aldrich and BOC-Science, respectively. Samples powders were placed onto a silicon substrate, shaped in order to guarantee the optimal x-ray path length L, such that it matches the photoelectric absorption length, $L = \mu^{-1}$, where μ is the absorption coefficient. The silicon substrate was beforehand covered with a 20 nm aluminum layer to improve adhesion. The powders were slowly heated above their melting temperature T_m, while slowly spinning the substrate to improve thickness homogeneity. Once the sample was an homogeneous and well transparent liquid, the substrate was removed from the heater and self-cooled at 100 K/min to room temperature. During cooling the liquid freezes into a disordered glassy state at T_g. The thickness of the resulting glasses were several mm. In order to prevent potential moisture absorption, the samples were stored in vacuum sealed boxes and the experiment was performed under dynamic high vacuum condition (10^{-6} bar). Control experiments, in inert gas and ambient conditions using differential scanning calorimetry, confirm moisture absorption during processing was negligible. The IXS experiment was carried out at the beam line ID28 of the European Synchrotron Radiation Facility (ESRF). Measurements of the scattered intensity at fixed scattering angles, and therefore fixed exchanged momentum Q values, were performed at room
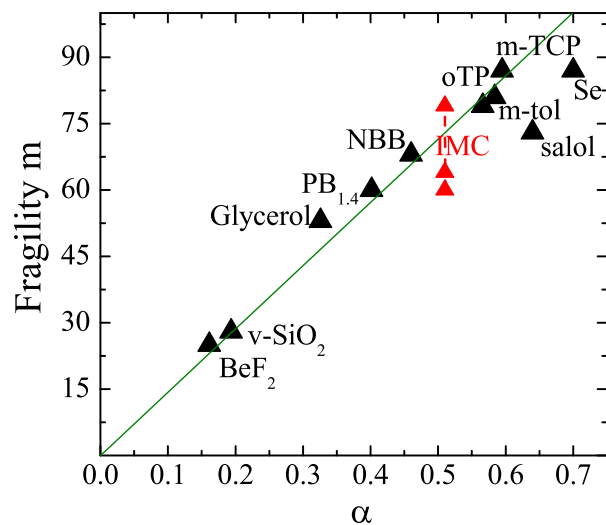
Figure 5 | Correlation plot of the kinetic fragility m and the α parameter of the non-ergodicity factor for several glassy systems. Three different experimental estimations of fragility available in literature are reported for IMC, ranging from 60 to 79[3,47,48].

temperature ($T = 300\ K$). An eight-analyzer bench, operating in horizontal scattering geometry, allowed the simultaneous collection of spectra at eight different values of Q. For both samples, the explored momentum-region extended from 1 up to 14.6 nm^{-1} thus reaching the position, Q_p, of the main peak in the diffraction pattern of both samples. The Q resolution determined by slits placed in front of the analyzer was set to 0.25 nm^{-1}. The scanned energy range was $-23 \le \hbar\omega \le 23\ meV$, where ω is the energy transfer such that $\hbar\omega = E_0 - E$, with E_0 and E being the energy of the incident (23.725 eV) and the scattered x-ray photon; each scan took approximately 480 min. Using the (12 12 12) reflection for the Si monochromator and crystal analyzers the overall energy resolution was 1.4 meV, the FWFM of the green line in Fig. 2 super-imposed to the elastic peak. The fitting function adopted to analyze the IXS spectra is the result of the convolution of the model function:

$$S(Q,\omega) = S(Q)\left[\delta(\omega)f_Q + \frac{(1-f_Q)}{\pi}\frac{\Omega(Q)^2\Gamma(Q)}{\left[\omega^2 - \Omega(Q)^2\right]^2 + \omega^2\Gamma^2(Q)}\right]\frac{\hbar\omega/(k_B T)}{1-e^{\hbar\omega/(k_B T)}} \quad (6)$$

with the instrument resolution. The two terms in eq.6 represent respectively the elastic and inelastic part of the spectra, where Ω defines the position of the inelastic peaks and Γ their widths. The assumption of a delta function for the elastic component is justified because the experimental data in the quasi-elastic region do not show any broadening compared to the instrument resolution. The inelastic component is described by a damped harmonic oscillator that is the solution of the generalized hydrodynamics using a Markovian memory function, i.e. assuming instantaneous relaxation of the molecular vibrations. This has been shown to be appropriate for the glassy state[45]. In order to account for the quantum nature of the probed excitations, we multiplied the function by the Bose factor such that it is adapted to satisfy the detailed balance condition.

1. Murdande, S. B., Pikal, M. J., Shanker, R. M. & Bogner, R. H. Solubility advantage of amorphous pharmaceuticals, part 3: Is maximum solubility advantage experimentally attainable and sustainable? *J. Pharm. Sci.* **100**, 4349–4356 (2011).
2. Hancock, B. C. & Zografi, G. Characteristics and significance of the amorphous state in pharmaceutical systems. *J. Pharm. Sci.* **86**, 1–12 (1997).
3. Swallen, S. F. & Ediger, M. D. Self-diffusion of the amorphous pharmaceutical indomethacin near T$_g$. *Soft Matter* **7**, 10339–10344 (2011).
4. Gupta, P., Chawla, G. & Bansal, A. K. Physical stability and solubility advantage from amorphous celecoxib: the role of thermodynamic quantities and molecular mobility. *Mol. Pharm.* **1**, 406–413 (2004).
5. Grzybowska, K. *et al.* Molecular Dynamics and Physical Stability of Amorphous Anti-Inflammatory Drug: Celecoxib. *J. Phys. Chem. B* **114**, 12792–12801 (2010).
6. Chawla, G., Gupta, P., Thilagavathi, R., Chakraborti, A. K. & Bansal, A. K. Characterization of solid-state forms of celecoxib. *Eur. J. Pharm. Sci.* **20**, 305–317 (2003).
7. Paradkar, A. R., Chauhan, B., Yamamura, S. & Pawar, A. P. Preparation and Characterization of Glassy Celecoxib. *Drug. Dev. Ind. Pharm.* **29**, 739–744 (2003).
8. Zeller, R. C. & Pohl, R. O. Thermal Conductivity and Specific Heat of Noncrystalline Solids. *Phys. Rev. B* **4**, 2029–2041 (1971).
9. Binder, K. & Kob, W. *Glassy Materials And Disordered Solids: An Introduction to Their Statistical Mechanics.* (World Scientific, 2005).
10. Schulte, A., Schirmacher, W., Schmid, B. & Unruh, T. Inelastic neutron and low-frequency Raman scattering in niobium-phosphate glasses: the role of spatially fluctuating elastic and elasto-optic constants. *J. Phys. Condens. Matter* **23**, 254212 (2011).
11. Schmid, B. & Schirmacher, W. Raman scattering and the low-frequency vibrational spectrum of glasses. *Phys. Rev. Lett* **100**, 137402 (2008).
12. Bove, L. E. *et al.* Brillouin neutron scattering of v-GeO$_2$. *Europhys. Lett.* **71**, 563–569 (2005).
13. Marruzzo, A., Köhler, S., Fratalocchi, A., Ruocco, G. & Schirmacher, W. Vibrational anomalies and marginal stability of glasses. *Eur. Phys. J.* **216**, 83–93 (2013).
14. Singh, S., Ediger, M. D. & de Pablo, J. J. Ultrastable glasses from in silico vapour deposition. *Nature Materials* **12**, 139–144 (2013).
15. Derlet, P. M., Maaβ, R. & Löffler, J. F. The Boson peak of model glass systems and its relation to atomic structure. *Eur. Phys. J. B* **85**, 1–20 (2012).
16. Marruzzo, A., Schirmacher, W., Fratalocchi, A. & Ruocco, G. Heterogeneous shear elasticity of glasses: the origin of the boson peak. *Sci. Rep.* **3**, 1407 (2013).
17. Zanatta, M., Armellini, C., Fontana, A. & Rossi, F. Temperature evolution of the boson peak and Debye scaling in vitreous B$_2$O$_3$. 12th International Workshop on Complex Systems: Andalo (Trento) Italy, 15–18 March 2010.
18. Sette, F., Krisch, M. H., Masciovecchio, C., Ruocco, G. & Monaco, G. Dynamics of Glasses and Glass-Forming Liquids Studied by Inelastic X-ray Scattering. *Science* **280**, 1550–1555 (1998).
19. Rayleigh, J. W. S. *The theory of sound* (Dover Publications, 1976).
20. Maris, H. J. *Physical Acoustics.* (ed. Mason, W. & Thurston, R.) vol. **8**, 279–345 (Academic Press, New York 1971).
21. Ferrante, C. *et al.* Acoustic dynamics of network-forming glasses at mesoscopic wavelengths. *Nat. Commun.* **4**, 1793 (2013).
22. Rufflé, B., Guimbretière, G., Courtens, E., Vacher, R. & Monaco, G. Glass-Specific Behavior in the Damping of Acousticlike Vibrations. *Phys. Rev. Lett.* **96**, 045502 (2006).
23. Ruocco, G., Matic, A., Scopigno, T. & Yannopoulos, S. N. Comment on "glass-specific behavior in the damping of acousticlike vibrations" *Phys. Rev. Lett.* **98**, 079601 (2007).
24. Shintani, H. & Tanaka, H. Universal link between the boson peak and transverse phonons in glass. *Nature Materials* **7**, 870–877 (2008).
25. Schober, H. R. Vibrations and relaxations in a soft sphere glass: boson peak and structure factors. *J. Phys. Condens. Matter* **16**, S2659 (2004).
26. Monaco, G. & Mossa, S. Anomalous properties of the acoustic excitations in glasses on the mesoscopic length scale. *PNAS* **106**, 16907–16912 (2009).
27. Scopigno, T., Ruocco, G., Sette, F. & Monaco, G. Is the Fragility of a Liquid Embedded in the Properties of Its Glass? *Science* **302**, 849–852 (2003).
28. Scopigno, T., Cangialosi, D. & Ruocco, G. Universal relation between viscous flow and fast dynamics in glass-forming materials. *Phys. Rev. B* **81**, 100202 (2010).
29. Niss, K. *et al.* Glassy properties and viscous slowing down: An analysis of the correlation between nonergodicity factor and fragility. *J. Chem. Phys.* **129**, 194513 (2008).
30. Böhmer, R., Ngai, K. L., Angell, C. A. & Plazek, D. J. Correlations of the nonexponentiality and state dependence of mechanical relaxations with bond connectivity in Ge-As-Se supercooled liquids. *J. Chem. Phys.* **99**, 4201–4209 (1993).
31. Angell, C. A. Structural instability and relaxation in liquid and glassy phases near the fragile liquid limit. *Journal of Non-Crystalline Solids* **102**, 205–221 (1988).
32. Yoshioka, S. & Aso, Y. Correlations between molecular mobility and chemical stability during storage of amorphous pharmaceuticals. *J. Pharm. Sci.* **96**, 960–981 (2007).
33. Baird, J. A., Santiago-Quinonez, D., Rinaldi, C. & Taylor, L. S. Role of viscosity in influencing the glass-forming ability of organic molecules from the undercooled melt state. *Pharm. Res.* **29**, 271–284 (2012).
34. Karmwar, P. *et al.* Investigations on the effect of different cooling rates on the stability of amorphous indomethacin. *Eur. J. Pharm. Sci.* **44**, 341–350 (2011).
35. Yu, L. Amorphous pharmaceutical solids: preparation, characterization and stabilization. *Adv. Drug. Deliv. Rev.* **48**, 27–42 (2001).
36. Yoshioka, M., Hancock, B. C. & Zografi, G. Crystallization of indomethacin from the amorphous state below and above its glass transition temperature. *Journal of pharmaceutical sciences* **83**, 1700–1705 (1994).
37. Kearns, K. L., Still, T., Fytas, G. & Ediger, M. D. High-Modulus Organic Glasses Prepared by Physical Vapor Deposition. *Advanced Materials* **22**, 39–42 (2010).
38. Ruocco, G. *et al.* Relaxation Processes in Harmonic Glasses? *Phys. Rev. Lett.* **84**, 5788–5791 (2000).
39. Bryk, T. & Mryglod, I. Concentration fluctuations and boson peak in a binary metallic glass: A generalized collective modes study. *Phys. Rev. B* **82**, 174205 (2010).
40. Götze, W. & Mayr, M. R. Evolution of vibrational excitations in glassy systems. *Phys. Rev. E* **61**, 587 (2000).
41. Monaco, G. & Giordano, V. M. Breakdown of the Debye approximation for the acoustic modes with nanometric wavelengths in glasses. *PNAS* **106**, 3659–3663 (2009).
42. Ruta, B. *et al.* Acoustic excitations in glassy sorbitol and their relation with the fragility and the boson peak. *J. Chem. Phys.* **137**, 214502 (2012).
43. Ruzicka, B. *et al.* Evidence of anomalous dispersion of the generalized sound velocity in glasses. *Phys. Rev. B* **69**, 100201 (2004).
44. Taraskin, S. N. & Elliott, S. R. Low-frequency vibrational excitations in vitreous silica: the Ioffe-Regel limit. *J. Phys. Condens. Matter* **11**, A219 (1999).
45. Scopigno, T., Ruocco, G. & Sette, F. Microscopic dynamics in liquid metals: the experimental point of view. *Rev. Mod. Phys.* **77**, 881–933 (2005).
46. Rufflé, B., Guimbretière, G., Courtens, E., Vacher, R. & Monaco, G. Glass-Specific Behavior in the Damping of Acousticlike Vibrations. *Phys. Rev. Lett.* **96**, 045502 (2006).
47. Ramos, J. J. M., Correia, N. T., Taveira-Marques, R. & Collins, G. The activation energy at Tg and the fragility index of indomethacin, predicted from the influence of the heating rate on the temperature position and on the intensity of thermally stimulated depolarization current peak. *Pharm. Res.* **19**, 1879–1884 (2002).
48. Correia, N. T., Ramos, J. J., Descamps, M. & Collins, G. Molecular mobility and fragility in indomethacin: a thermally stimulated depolarization current study. *Pharm. Res.* **18**, 1767–1774 (2001).

Acknowledgments

Author contributions

T.S. conceived and supervised the research. E.A.A.P., C.R.-T., M.K and T.S. performed the experiment. E.A.A.P. analysed the data. C.R.-T. and J.R.-V. provided and characterized the samples. E.A.A.P. and T.S. wrote the manuscript. All the authors participated to the discussion of the results and commented on the manuscript.

Additional information